

## Hard probes in heavy ion collisions: current status and prospects for application of QCD evolution techniques

Ivan Vitev

*Theoretical Division, Los Alamos National Laboratory, Mail Stop B283  
Los Alamos, NM 87545, U.S.A.  
ivitev@lanl.gov*

Received Day Month Year  
Revised Day Month Year  
Published Day Month Year

In the past decade the observation of cross section modification for leading hadrons, heavy flavor and two particle correlations in heavy ion collisions has provided important insights into the dynamics of parton propagation in dense strongly-interacting matter. The development of the theory of reconstructed jets and related experimental measurements have further shed light on the characteristics of in-medium parton showers. So far, experimental results from ultra-relativistic nuclear collisions at RHIC and LHC have been analyzed in the framework of parton energy loss, where the precision of the theoretical predictions cannot be systematically improved. Only recently have higher order calculations and applications of resummation and evolution to heavy ion collisions begun to emerge. Several examples of such advances are discussed in these proceedings.

*Keywords:* Heavy ion collisions; jets; resummation.

PACS numbers:12.38.-t, 12.38.Bx, 12.38.Cy, 24.85.+p

### 1. Introduction

In this brief overview, emergent approaches that aim at increasing the theoretical precision in the evaluation of hard probes observables in heavy ion collisions are discussed. It was realized more than twenty years ago that in the ambience of strongly-interacting matter the cross sections for high transverse momentum hadron production will be attenuated. This phenomenon, dubbed "jet quenching", has attracted tremendous attention from the theoretical and experimental communities<sup>1</sup> at the Relativistic Heavy Ion Collider (RHIC) and the Large Hadron Collider (LHC) and has subsequently been extended to heavy flavor production, particle correlations and, most importantly, reconstructed jet observables. Within the framework of the traditional parton energy loss approach, however, the accuracy of such theoretical analyses cannot be systematically improved. Recent advances in the theory

This is an Open Access article published by World Scientific Publishing Company. It is distributed under the terms of the Creative Commons Attribution 3.0 (CC-BY) License. Further distribution of this work is permitted, provided the original work is properly cited.

of in-medium parton shower formation allow us to overcome this limitation and to unify our understanding of energetic particle and jet production in hadronic and nuclear collisions. Next-to-leading order calculations and application of evolution techniques for deep inelastic scattering and heavy ion collisions at RHIC and the LHC are described in more detail in <sup>2,3,4,5,6,7</sup>. A briefer overview of soft-collinear effective theory (SCET) and discussion of the connection between perturbative QCD (pQCD) and SCET resummation techniques can be found in <sup>8,9</sup>. For applications to heavy ion collisions, SCET has been extended to include Glauber modes <sup>10,11</sup>. The progress toward better understanding of hard probes in heavy ion collisions, with emphasis on future directions, is concisely reviewed below.

## 2. Parton propagation in matter and energy loss

Given the significance of understanding the production of large transverse momentum particles and jets in the ambiance of the QGP, several theoretical formalisms were developed to evaluate the energy loss of quarks and gluons as they propagate through the medium <sup>12,13,14,15</sup>. As an example, we present below the Guuylassy-Levai-Vitev (GLV) reaction operator approach where the fully differential medium induced gluon bremsstrahlung intensity is obtained as a series over the multiple scattering correlations in the medium. For gluons with momentum  $k = [xp^+, \mathbf{k}^2/xp^+, \mathbf{k}]$  resulting from the sequential interactions of a fast parton with momentum  $p = [p^+, 0, \mathbf{0}]$  can be written as

$$\begin{aligned}
x \frac{dN_g}{dx d^2\mathbf{k}} &= \sum_{n=1}^{\infty} x \frac{dN_g^{(n)}}{dx d^2\mathbf{k}} = \sum_{n=1}^{\infty} \frac{C_R \alpha_s}{\pi^2} \prod_{i=1}^n \int_0^{L - \sum_{a=1}^{i-1} \Delta z_a} \frac{d\Delta z_i}{\lambda_g(i)} \\
&\int d^2\mathbf{q}_i \left[ \sigma_{el}^{-1}(i) \frac{d\sigma_{el}(i)}{d^2\mathbf{q}_i} - \delta^2(\mathbf{q}_i) \right] \left( -2 \mathbf{C}_{(1, \dots, n)} \cdot \sum_{m=1}^n \mathbf{B}_{(m+1, \dots, n)(m, \dots, n)} \right. \\
&\times \left. \left[ \cos \left( \sum_{k=2}^m \omega_{(k, \dots, n)} \Delta z_k \right) - \cos \left( \sum_{k=1}^m \omega_{(k, \dots, n)} \Delta z_k \right) \right] \right), \quad (1)
\end{aligned}$$

where  $\sum_2^1 \equiv 0$  is understood. In the small angle eikonal limit  $x = k^+/p^+ \approx \omega/E$ . In Eq. (1) the color current propagators are denoted by

$$\begin{aligned}
\mathbf{C}_{(m, \dots, n)} &= \frac{1}{2} \nabla_{\mathbf{k}} \ln (\mathbf{k} - \mathbf{q}_m - \dots - \mathbf{q}_n)^2 \\
\mathbf{B}_{(m+1, \dots, n)(m, \dots, n)} &= \mathbf{C}_{(m+1, \dots, n)} - \mathbf{C}_{(m, \dots, n)} \quad . \quad (2)
\end{aligned}$$

The momentum transfers  $\mathbf{q}_i$  are distributed according to a normalized elastic differential cross section,

$$\sigma_{el}(i)^{-1} \frac{d\sigma_{el}(i)}{d^2\mathbf{q}_i} = \frac{\mu^2(i)}{\pi(\mathbf{q}_i^2 + \mu^2(i))^2}, \quad (3)$$

which models scattering by soft partons with a thermally generated Debye screening mass  $\mu(i)$ . For gluon dominated bulk soft matter  $\sigma_{el}(i) \approx \frac{9}{2} \pi \alpha_s^2 / \mu^2(i)$  and  $\lambda_g(i) =$

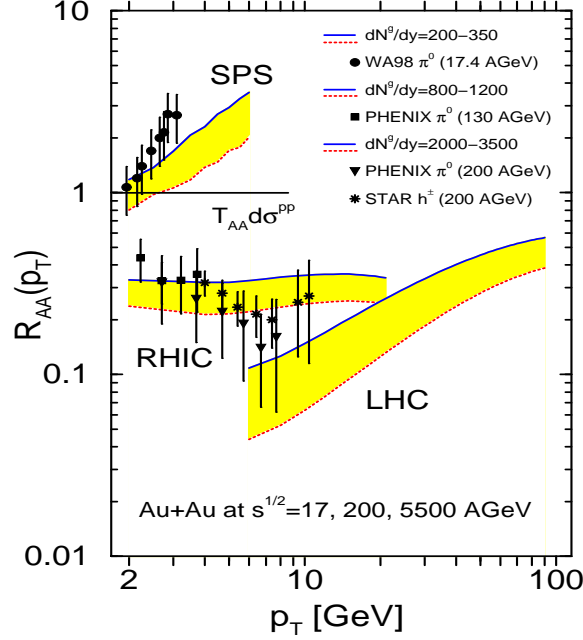


Fig. 1. The suppression/enhancement ratio  $R_{AA}(p_T)$  ( $A = B = Au$ ) for neutral pions at  $\sqrt{s_{NN}} = 17, 200, 5500$  GeV. Solid (dashed) lines correspond to the smaller (larger) effective initial gluon rapidity densities at given  $\sqrt{s}$  that drive parton energy loss. Data on  $\pi^0$  production in central  $Pb+Pb$  at  $\sqrt{s_{NN}} = 17.4$  GeV from WA98 and in central  $Au+Au$  at  $\sqrt{s_{NN}} = 130$  GeV, as well as *preliminary* data at 200 GeV from PHENIX and  $h^\pm$  central/peripheral data from STAR are shown. The sum of estimated statistical and systematic errors are indicated.

$1/\sigma_{el}(i)\rho(i)$ . The characteristic path length dependence of the non-Abelian energy loss in Eq. (1) comes from the interference phases and is differentially controlled by the inverse formation times,

$$\omega_{(m,\dots,n)} = \frac{(\mathbf{k} - \mathbf{q}_m - \dots - \mathbf{q}_n)^2}{2xE}, \quad (4)$$

and the separations of the subsequent scattering centers  $\Delta z_k = z_k - z_{k-1}$ . It is the non-Abelian analogue of the Landau-Pomeranchuk-Migdal destructive interference effect in QED, which, for a static plasma, up to kinematic corrections yields the following parametric behavior with respect to the energy and path length of the parton:  $\Delta E \sim L^2 \ln E$ .

### 2.1. The energy loss approach to jet quenching

Should an energy loss approach be adopted, it is important to realize that the soft gluon emission limit must be consistently implemented. If the fractional energy loss becomes significant, it is carried away through multiple gluon bremsstrahlung. In the independent Poisson gluon emission limit, we can construct the probability

density  $P_c(\epsilon)$  of this fractional energy loss  $\epsilon = \sum_i \omega_i/E \approx \sum_i k_i^+/p^+$ , such that:

$$\int_0^1 d\epsilon P(\epsilon) = 1, \quad \int_0^1 d\epsilon \epsilon P(\epsilon) = \left\langle \frac{\Delta E}{E} \right\rangle. \quad (5)$$

A more detailed discussion is given in <sup>1</sup>. If a parton loses this energy fraction  $\epsilon$  during its propagation in the QGP to escape with momentum  $p_{T_c}^{\text{quench}}$ , immediately after the hard collision  $p_{T_c} = p_{T_c}^{\text{quench}}/(1 - \epsilon)$ . Noting the additional Jacobian  $|dp_{T_c}^{\text{quench}}/dp_{T_c}| = (1 - \epsilon)$ , the kinematic modification to the FFs due to energy loss is:

$$D_c^{\text{quench}}(z) = \int_0^{1-z} d\epsilon \frac{P_c(\epsilon)}{(1 - \epsilon)} D_c\left(\frac{z}{1 - \epsilon}\right), \quad (6)$$

and can be directly implemented in the evaluation of inclusive and tagged hadron production. Comparison of theoretical predictions for the nuclear modification factor for inclusive light hadron production, defined as

$$R_{AA}(p_T) = \frac{d\sigma_{AA}^h/dy d^2p_T}{\langle N_{\text{coll}} \rangle d\sigma_{pp}^h/dy d^2p_T}, \quad (7)$$

to experimental data is shown in Fig. 1. In Eq. (7)  $\langle N_{\text{coll}} \rangle$  is the average number of binary nucleon-nucleon collisions.

A wide variety of models for parton energy loss were employed to fit RHIC "jet quenching" measurements and theoretical predictions for the Pb+Pb run at the LHC were summarized in <sup>17</sup>. The majority of these calculations failed to describe the LHC inclusive particle suppression data <sup>18</sup>, in particular its  $p_T$  dependence, which Fig. 1 represents well. Although it was subsequently shown that many of the approaches can fit the data through model improvements and parameter adjustment, it is now clear that better understanding of the characteristics of the in-medium and improved theoretical precision of the calculations is necessary.

## 2.2. The theory of reconstructed jets in heavy ion collisions

Suppression of the reconstructed jet cross sections and modification of the jet substructure observables in heavy ion collisions are sensitive signatures of the QGP-modified parton dynamics. In particular, jet measurements in heavy ion collisions provide unique access to the longitudinal and transverse structure of the medium induced parton shower that is not possible through leading particle or particle correlations analyses. For a jet reconstruction parameter  $R$  one can evaluate from Eq. (1) the part of the fractional energy loss  $\epsilon_i$  that is simply redistributed inside the jet for a parent parton "i"

$$f(R_i, p_{T_i}^{\text{min}})_{q,g} = \frac{\int_0^{R_i} dr \int_{p_{T_i}^{\text{min}}}^{E_{T_i}} d\omega \frac{dI_{q,g}^{\text{rad}}(i)}{d\omega dr}}{\int_0^{R_i} dr \int_0^{E_{T_i}} d\omega \frac{dI_{q,g}^{\text{rad}}(i)}{d\omega dr}}. \quad (8)$$

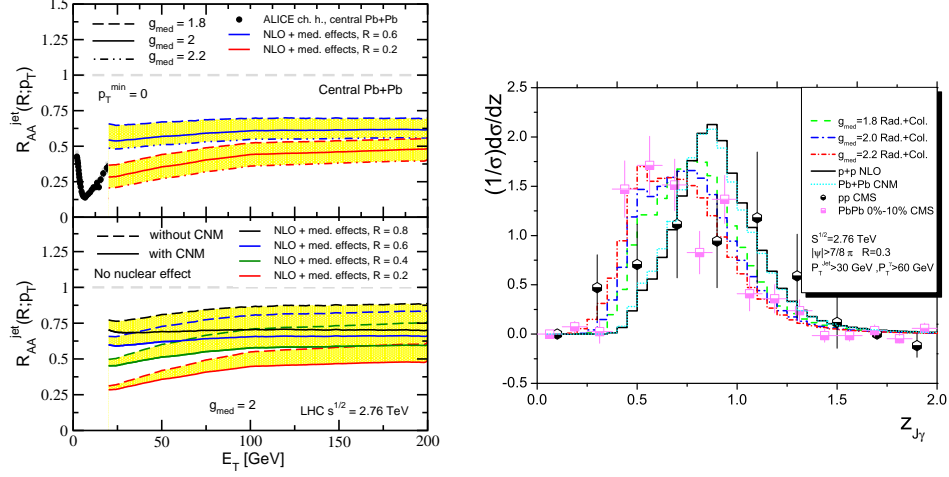


Fig. 2. Left panel: the  $E_T$  dependence of the nuclear modification factor for different jet cone sizes  $R = 0, 2, 0.6$  is calculated in central Pb+Pb collisions at the LHC  $\sqrt{s_{NN}} = 2.76$  TeV. Bands represent the variation in the coupling strength between the jet and the medium. The relative contribution of cold nuclear matter effects to  $R_{AA}$  is illustrated for  $R = 0.2, 0.4, 0.6, 0.8$ . Right panel: the momentum imbalance of photon tagged jets in p+p and A+A collisions is compared to CMS experimental data in p+p and Pb+Pb reactions.

Thus,  $f(R_i, p_{T_i}^{\min})_{q,g}$  plays a critical role in defining the contribution (or lack thereof if  $f(R_i, p_{T_i}^{\min})_{q,g} \rightarrow 0$ ) of the medium-induced bremsstrahlung to the jet. Note that in Eq. (8)  $p_{T_i}^{\min}$  is a parameter that can be used to simulate processes that can alter the energy of the jet beyond medium-induced bremsstrahlung, for example collisional energy loss.

The medium-modified jet cross section for jets per binary scattering is evaluated as

$$\frac{1}{\langle N_{\text{bin}} \rangle} \frac{d\sigma^{AA}(R)}{dy_1 dE_{T1}} = \sum_{q,g} \int_{\epsilon_1=0}^1 d\epsilon_1 \frac{P_{q,g}(\epsilon_1, E_{T1})}{(1 - [1 - f(R_1, p_{T1}^{\min})_{q,g}] \epsilon_1)} \frac{d\sigma_{q,g}^{\text{CNM,NLO}}(E'_{T1})}{dy_1 dE'_{T1}}. \quad (9)$$

In Eq. (9) the phase space Jacobian reads

$$|J_i(\epsilon_i)| = 1 / (1 - [1 - f(R_i, p_{T_i}^{\min})_{q,g}] \epsilon_i),$$

and  $E'_{T_i} = |J_i(\epsilon_i)| E_{T_i}$  in the argument of  $\sigma_{q,g}^{\text{CNM,NLO}}$ .

One of the most important theoretical predictions related to jet production in heavy ion collisions is the radius dependence of jet suppression<sup>19</sup>. It is illustrated in the left panel of Fig. 2 and arises from the broader angular distribution of the QGP-induced parton shower in comparison to the parton shower in the absence of the strongly-interacting medium. In the limit of small jet radii  $R \rightarrow 0$ , it approaches the level of suppression observed in inclusive particle production. This expectation is now confirmed by the ATLAS experimental data<sup>20</sup>. Further constraints on the

modification of the parton shower can be placed through electroweak boson tagging<sup>21</sup> and the change in the shape and magnitude of correlation distribution, such as the momentum imbalance  $z_J = p_{T\text{jet}}/p_{T\gamma,Z^0}$ . One such example is shown in the right panel of Fig. 2 and additional theoretical predictions for these channels have also been confirmed by LHC experimental data.

### 3. Resummation for hard probes in heavy ion collisions

The next step in improving the theory of leading particles and jets in heavy ion reactions is to employ resummation/evolution techniques where the theoretical control on the accuracy of the evaluation is much improved. An important step forward was the derivation of all medium-induced splitting functions beyond the soft-gluon (energy loss) approximation<sup>23</sup>.

#### 3.1. Evolution approach to leading particle production in $A+A$

A critical step in improving the jet quenching phenomenology is to understand the implication of the finite- $x$  corrections. Their implementation requires new theoretical methods, since in the large momentum fraction limit the leading parton can change flavor and the splitting process cannot be interpreted as energy loss. A natural language to capture this physics is that of the well-known Dokshitzer-Gribov-Lipatov-Altarelli-Parisi (DGLAP) evolution equations, which provide up to modified leading logarithmic accuracy. As a first application of the full medium-induced splitting kernels<sup>4,23</sup>, we revisit the evaluation of the nuclear modification factor  $R_{AA}$  for inclusive hadron production at high transverse momentum  $p_T$  (and rapidity  $y$ )<sup>5</sup>.

Given the success of the traditional jet quenching phenomenology, it is important to establish the connection between the evolution and energy loss approaches<sup>4,5</sup>. This can be achieved *only* in the soft gluon bremsstrahlung limit, where the two diagonal splitting functions  $P_{q\rightarrow qg}(z')$  and  $P_{g\rightarrow gg}(z')$  survive. branching is given by a plus function. The DGLAP evolution equations decouple and because the fragmentation functions  $D(z/z')$  are typically steeply falling with increasing  $p_T^{\text{hadron}}/p_T^{\text{parton}}$ , the main contribution comes predominantly from  $z' \approx 1$ . We expand the integrand in this limit, the analytical solution

$$D^{\text{med}}(z, Q) \approx e^{-(n(z)-1)\langle \frac{\Delta E}{E} \rangle_z - \langle N_g \rangle_z} D^{\text{vac}}(z, Q), \quad (10)$$

and shows explicitly that the vacuum evolution and the medium-induced evolution factorize. We have used the following definitions in the above formula:

$$\left\langle \frac{\Delta E}{E} \right\rangle_z = \int_0^{1-z} dx x \frac{dN}{dx}(x) \xrightarrow{z \rightarrow 0} \left\langle \frac{\Delta E}{E} \right\rangle, \quad \langle N_g \rangle_z = \int_{1-z}^1 dx \frac{dN}{dx}(x) \xrightarrow{z \rightarrow 1} \langle N_g \rangle, \quad (11)$$

where  $xdN/dx$  is the medium-induced gluon intensity distribution<sup>13</sup> and the connection to the traditional energy loss approach is evident.

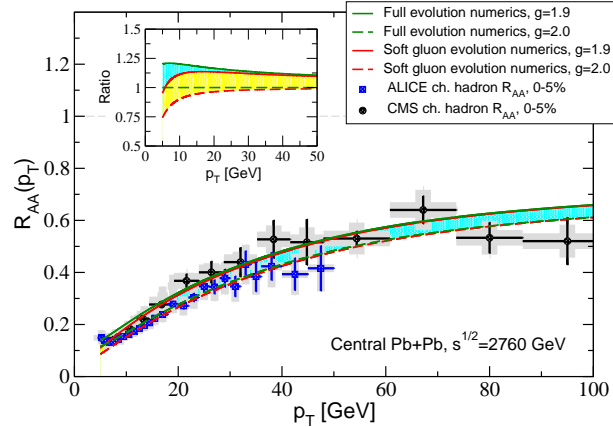


Fig. 3. Comparison between  $R_{AA}$  obtained with in-medium numerically evolved fragmentation functions using the full splitting kernels (cyan band) and their soft gluon limit (yellow band) to ALICE and CMS data. The upper and lower edges of the bands correspond to  $g = 1.9$  and  $g = 2.0$ , respectively.

Conversely, solving the DGLAP evolution equations with the full medium induced splitting functions allows us to unify the treatment of vacuum and medium-induced parton showers. It gives a very good description of the RHIC and LHC experimental data, as illustrated in Fig. 3. We find that the coupling between the jet and the medium can be constrained with better than 10% accuracy when the uncertainties that arise from the choice of method and the fit to the data are combined. The investigation of the medium-evolved fragmentation functions further reveals that significant improvement in the reliability of the theoretical predictions by using the approach described here can be obtained for more exclusive observables.

### 3.2. Jet shapes in hadronic collisions

The jet shape is a classic jet substructure observable that probes the average transverse energy profile inside a reconstructed jet. Given a jet with an axis  $\hat{n}$ , its integral and differential jet shapes,  $\Psi_J(r)$  and  $\psi_J(r)$ , are defined as follows,

$$\Psi_J(r) = \frac{\sum_{i, d_{i\hat{n}} < r} E_T^i}{\sum_{i, d_{i\hat{n}} < R} E_T^i}, \quad \psi_J(r) = \frac{d\Psi_J(r)}{dr}. \quad (12)$$

The studies of jet shapes in proton-proton collisions have served as precision tests of perturbative Quantum Chromodynamics (QCD). They have also recently become the baseline for studying the in-medium modification of parton showers in ultra-relativistic nucleus-nucleus collisions. The jet shape is a function of two angular parameters  $R$  and  $r$ , which can be at hierarchical scales. Its calculation suffers from large logarithms of the ratio between the two scales, and these phase space

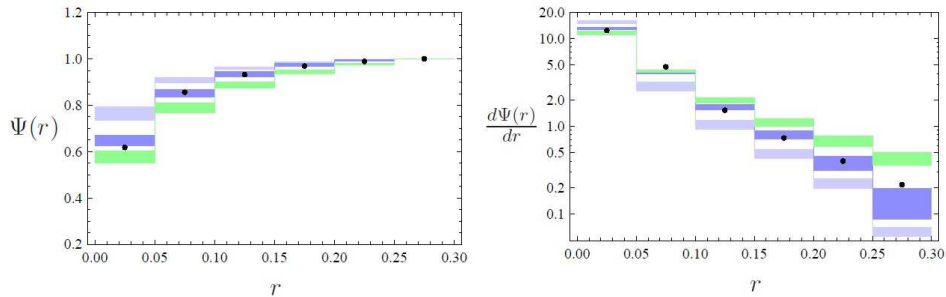


Fig. 4. The integral (left) and differential (right) jet shapes in proton-proton collisions with center of mass energy at  $\sqrt{s_{\text{NN}}} = 2.76$  TeV are plotted as a function of  $r$ , which is the angle from the jet axis. Jets are reconstructed using the anti- $k_T$  algorithm with  $R = 0.3$ . The cuts on the transverse momenta and rapidity of the jets ( $p_T^{\text{jet}} > 100$  GeV and  $0.3 < |y^{\text{jet}}| < 2$ ) are imposed. The dots are the CMS data with negligible experimental uncertainties. The shaded blue boxes are the LO (light) and NLL (dark) results for anti- $k_T$  jets, with the theoretical uncertainties estimated by varying the jet scales between  $\frac{1}{2}\mu_{j_R} < \mu < 2\mu_{j_R}$ . The NLL results agree with the data much better than the LO results. The shaded green boxes are the NLL results for cone jets, plotted as an illustration of the algorithm dependence in jet shapes.

logarithms can be conveniently resummed in the framework of soft-collinear effective theory (SCET). Early evaluation of jet shapes in heavy ion collisions<sup>24</sup> has predicted all qualitative features of the modification of this observable relative to p+p collisions, measured only recently in Pb+Pb reactions at the LHC<sup>25</sup>. At the same, time the need for quantitative improvement in theory is significant. Part of this improvement is a better evaluation of the  $\psi_J(r)$  p+p baseline.

The evaluation of jet shapes in the framework of SCET, up to power corrections from initial state radiation, was presented in<sup>6,7</sup>. The SCET calculations of the differential jet shapes  $\Psi_\omega(r)$  includes the one-loop jet energy functions, the two-loop cusp anomalous dimensions ( $\Gamma_0$  and  $\Gamma_1$ ) and the one-loop anomalous dimensions ( $\gamma_0^{q,g}$ ) of the jet energy functions, as well as the two-loop running of the strong coupling constant with  $\alpha_s(m_Z) = 0.1172$ . This will give us the precision formally at next-to-leading logarithmic order (NLL), including terms down to  $\alpha_s^n \ln^{2n-1} \frac{r}{R}$ .

Figure 4 shows the comparison between the LO and NLL calculations and the CMS measurement of the integral and differential jet shapes in proton-proton collisions at  $\sqrt{s_{\text{NN}}} = 2.76$  TeV. The shaded boxes are the theoretical uncertainties we estimate by varying the jet scales between  $\frac{1}{2}\mu_{j_R} < \mu < 2\mu_{j_R}$ . The LO calculation, due to its divergent nature, certainly can not describe the data and resummation becomes necessary. The results for cone jets are also shown to illustrate the algorithm dependence in jet shapes.

#### 4. Conclusions

These proceedings presented a brief overview of the evolution of medium-induced parton energy loss "jet quenching" applications from leading particles to jets. I dis-



cussed emergent approaches, based on resummation/evolution and modern effective theories of QCD, that aim at increasing the theoretical precision in the evaluation of hard probes observables in heavy ion collisions. These theoretical advances pave the way toward a unified treatment of vacuum and in-medium parton showers and a common approach to understanding jet production in particle and high-energy nuclear physics.

### Acknowledgments

I. Vitev is supported by the US Department of Energy, Office of Science, Office of Nuclear Physics and Office of Fusion Energy Sciences and in part by the LDRD program at LANL.

### References

1. M. Gyulassy, I. Vitev, X. N. Wang and B. W. Zhang, In \*Hwa, R.C. (ed.) et al.: Quark gluon plasma\* 123-191 [nucl-th/0302077]; references therein.
2. H. Xing, *These proceedings*.
3. Z. B. Kang, E. Wang, X. N. Wang and H. Xing, arXiv:1409.1315 [hep-ph].
4. G. Ovanessian, *These proceedings*, arXiv:1410.4157 [hep-ph].
5. Z. B. Kang, R. Lashof-Regas, G. Ovanessian, P. Saad and I. Vitev, arXiv:1405.2612 [hep-ph].
6. Y.-T. Chien, *These proceedings*.
7. Y. T. Chien and I. Vitev, arXiv:1405.4293 [hep-ph].
8. C. Lee, *These proceedings*, arXiv:1410.4216 [hep-ph].
9. L. G. Almeida, S. D. Ellis, C. Lee, G. Sterman, I. Sung and J. R. Walsh, JHEP **1404**, 174 (2014) [arXiv:1401.4460 [hep-ph]].
10. A. Idilbi and A. Majumder, Phys. Rev. D **80**, 054022 (2009) [arXiv:0808.1087 [hep-ph]].
11. G. Ovanessian and I. Vitev, JHEP **1106**, 080 (2011) [arXiv:1103.1074 [hep-ph]].
12. R. Baier, Y. L. Dokshitzer, A. H. Mueller and D. Schiff, Nucl. Phys. B **531**, 403 (1998) [hep-ph/9804212].
13. M. Gyulassy, P. Levai and I. Vitev, Nucl. Phys. B **594**, 371 (2001) [nucl-th/0006010].
14. X. N. Wang and X. f. Guo, Nucl. Phys. A **696**, 788 (2001) [hep-ph/0102230].
15. P. B. Arnold, G. D. Moore and L. G. Yaffe, JHEP **0206**, 030 (2002) [hep-ph/0204343].
16. I. Vitev and M. Gyulassy, Phys. Rev. Lett. **89**, 252301 (2002) [hep-ph/0209161].
17. N. Armesto, arXiv:0903.1330 [hep-ph]; references therein.
18. S. Chatrchyan *et al.* [CMS Collaboration], Eur. Phys. J. C **72**, 1945 (2012) [arXiv:1202.2554 [nucl-ex]]; references therein
19. Y. He, I. Vitev and B. W. Zhang, Phys. Lett. B **713**, 224 (2012) [arXiv:1105.2566 [hep-ph]].
20. G. Aad *et al.* [ATLAS Collaboration], Phys. Lett. B **719**, 220 (2013) [arXiv:1208.1967 [hep-ex]].
21. R. B. Neufeld, I. Vitev and B.-W. Zhang, Phys. Rev. C **83**, 034902 (2011) [arXiv:1006.2389 [hep-ph]].
22. W. Dai, I. Vitev and B. W. Zhang, Phys. Rev. Lett. **110**, 142001 (2013) [arXiv:1207.5177 [hep-ph]]; references therein.
23. G. Ovanessian and I. Vitev, Phys. Lett. B **706**, 371 (2012) [arXiv:1109.5619 [hep-ph]].

24. I. Vitev, S. Wicks and B. W. Zhang, JHEP **0811**, 093 (2008) [arXiv:0810.2807 [hep-ph]].
25. S. Chatrchyan *et al.* [CMS Collaboration], Phys. Lett. B **730**, 243 (2014) [arXiv:1310.0878 [nucl-ex]].